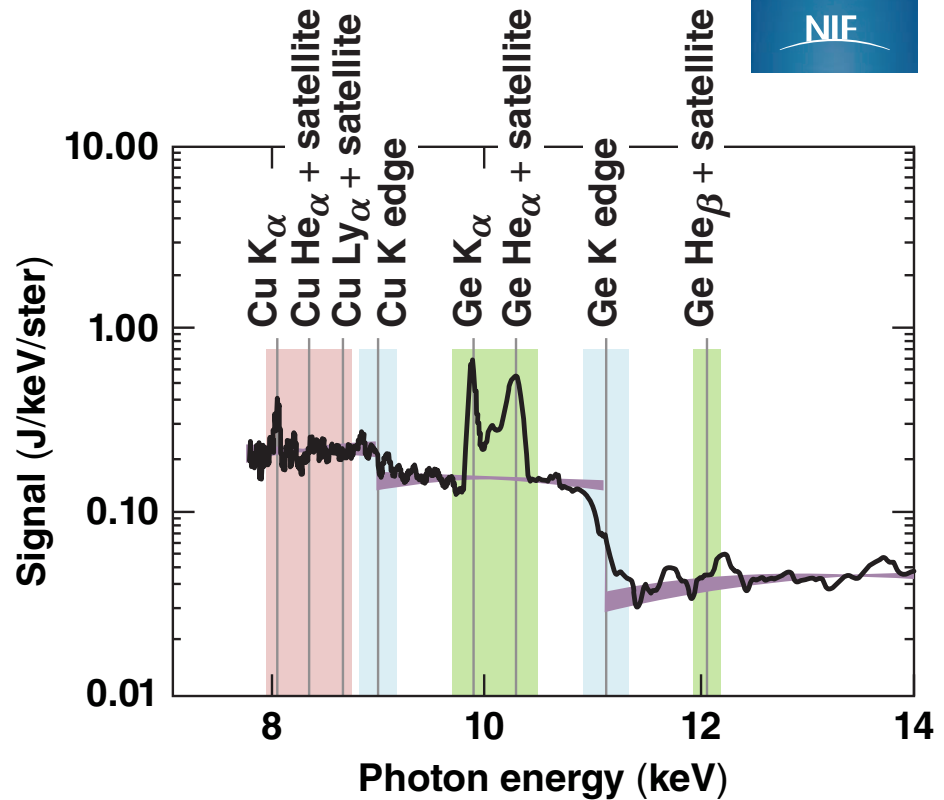
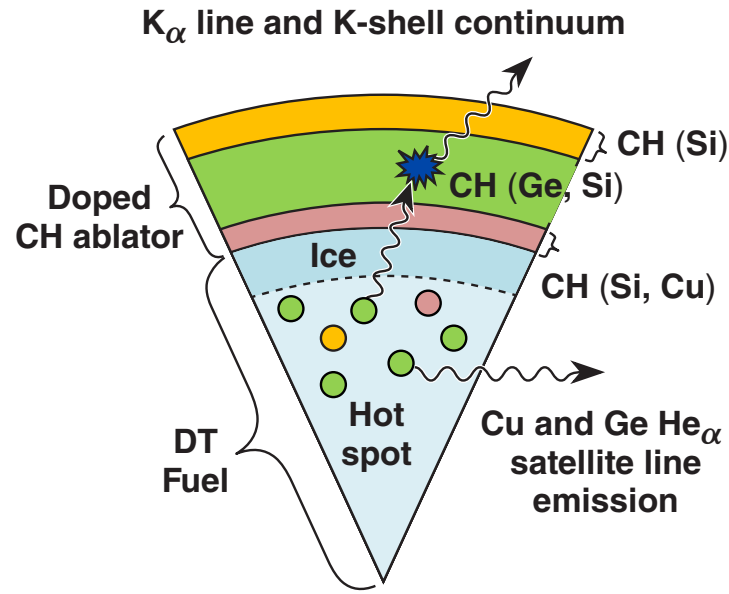


X-Ray Spectroscopy of Implosions at the National Ignition Facility



S. P. Regan
University of Rochester
Laboratory for Laser Energetics

44th Annual Anomalous
Absorption Conference
Estes Park, CO
8–13 June 2014

The hot-spot and compressed shell of ignition-scale implosions are diagnosed with x-ray spectroscopy



- Ablator mass mixed into the hot spot is inferred from the intensity of the $\text{He}_\alpha +$ satellite line emission of mid-Z ablator dopants*,**
- The origin of the hot-spot mix mass is investigated using Cu and Ge dopants placed at different radial locations in the ablator***
- The compressed-shell conditions are inferred from the absorption of x rays from the hot spot by the compressed Ge-doped CH
- Hydrodynamic mixing is predicted to increase the T_e and n_e of the Ge-doped CH in the compressed shell

These time-integrated measurements will be extended with streaked x-ray spectroscopy using the National Ignition Facility (NIF) x-ray spectrometer (NXS).

*B. A. Hammel et al., High Energy Density Phys. 6, 171(2010).

**S. P. Regan et al., Phys. Plasmas 19, 056307 (2012).

***S. P. Regan et al., Phys. Rev. Lett. 111, 045001 (2013).

Collaborators



R. Epstein, R. L. McCrory, D. D. Meyerhofer, and T. C. Sangster

**University of Rochester
Laboratory for Laser Energetics**

**B. A. Hammel, L. J. Suter, H. A. Scott, M. A. Barrios, D. K. Bradley, D. A. Callahan, C. Cerjan,
G. W. Collins, T. Dittrich, S. N. Dixit, T. Doeppner, M. J. Edwards, K. B. Fournier, S. Glenn,
S. W. Haan, A. Hamza, D. Hinkel, O. A. Hurricane, C. A. Iglesias, N. Izumi, O. S. Jones,
O. L. Landen, T. Ma, A. J. Mackinnon, N. B. Meezan, A. Pak, H.-S. Park, P. K. Patel, J. Ralph,
B. A. Remington, V. A. Smalyuk, P. T. Springer, R. P. J. Town, and B. G. Wilson**

Lawrence Livermore National Laboratory, Livermore, CA

S. H. Glenzer

SLAC National Accelerator Laboratory, Menlo Park, CA

I. E. Golovkin and J. J. MacFarlane

Prism Computational Sciences, Madison, WI

H. Huang, J. Jaquez, J. D. Kilkenny, and A. Nikroo
General Atomics, San Diego, CA

J. L. Kline and G. A. Kyrala

Los Alamos National Laboratory, Los Alamos, NM

R. C. Mancini

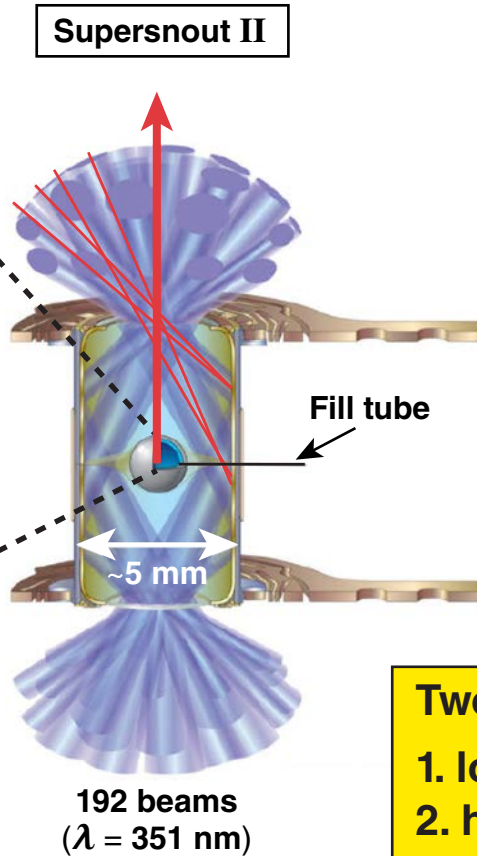
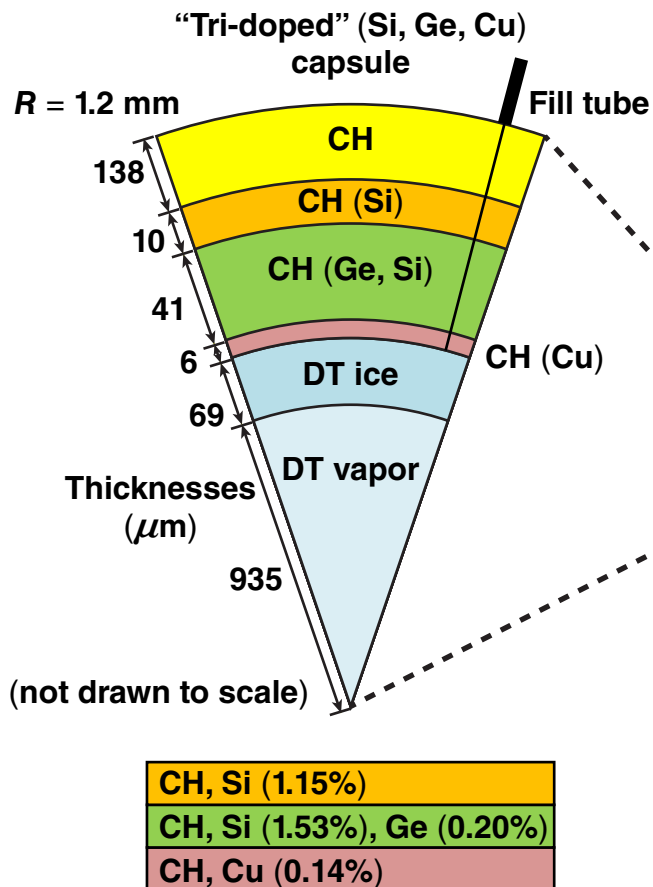
University Of Nevada, Reno, NV

X-ray spectroscopy of implosions at the NIF



- **NIF implosion experiment**
 - Supersnout II
- **X-ray emission spectroscopy of the hot spot**
 - hot-spot mix
- **X-ray absorption spectroscopy of the compressed shell**
 - hydrodynamic mixing of shell layers
- **Future direction**
 - streaked x-ray spectroscopy on NIF
- **Conclusion**

Ignition-scale capsules with trace amounts of Ge and Cu are imploded with hohlraums on the NIF



- $E_{\text{UV}} = 1.3 \text{ MJ to } 1.8 \text{ MJ}$
- CH ablator
- Si dopant is a preheat shield
- Ge/Cu dopants are used for emission/absorption x-ray spectroscopy
- adiabat ($\alpha = P_{\text{fuel}}/P_{\text{Fermi}}$) is set by the laser drive

Two types of implosion are studied:
1. low-adiabat ($\alpha \sim 1$)^{*}
2. high-adiabat ($\alpha \sim 3$)^{**}

*M. J. Edwards et al., Phys. Plasmas **20**, 070501 (2013).

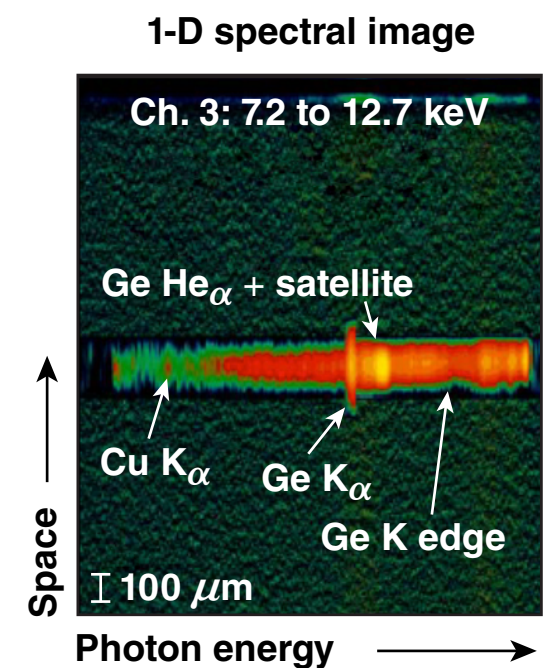
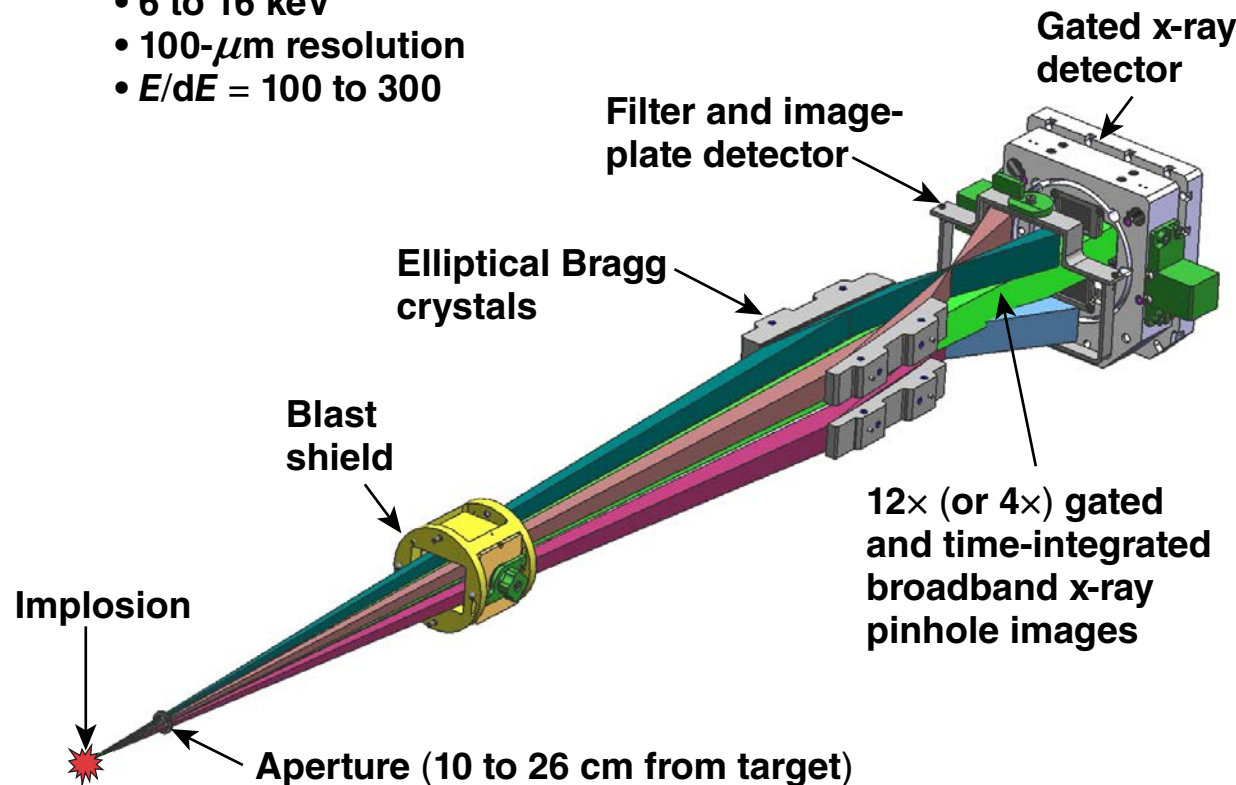
O. A. Hurricane., Nature **506, 343 (2014).

A time-integrated, 1-D imaging spectrometer was used to record x-ray spectra in the 6- to 16-keV range



Supersnout II

- 6 to 16 keV
- 100- μ m resolution
- $E/dE = 100$ to 300



Supersnout II combines 1-D spectral imaging and broadband gated and time-integrated x-ray imaging in a single snout.

The ablation-surface instability* and the inner-shell deceleration instability initiate mix at different times and locations



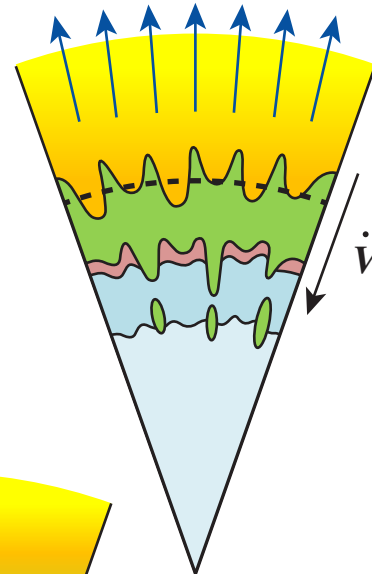
- Find the instability criterion

$$\vec{\nabla}P \cdot \vec{\nabla}\rho < 0$$

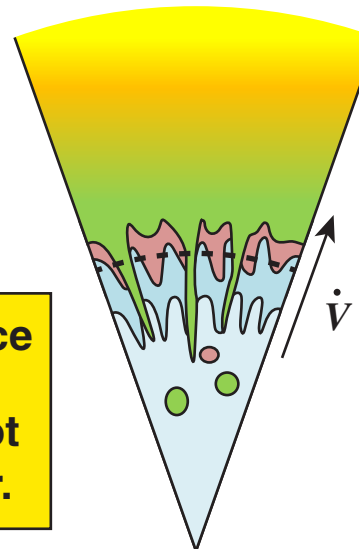
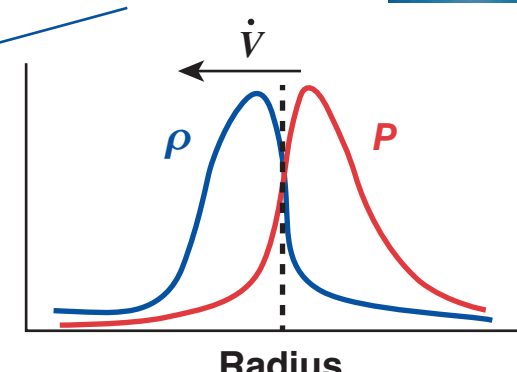
satisfied near the dashed lines

CH (Si)
CH (Ge, Si)
CH (Cu)

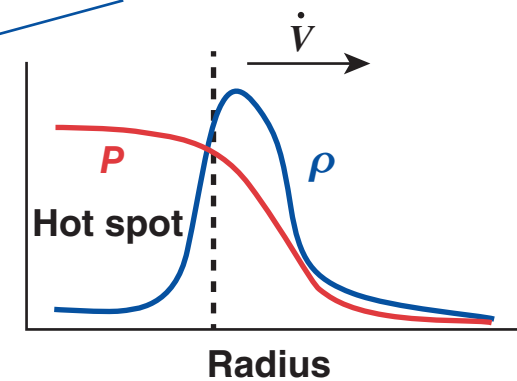
The ablation surface reaches the Ge-doped layer, but not the Cu-doped layer.



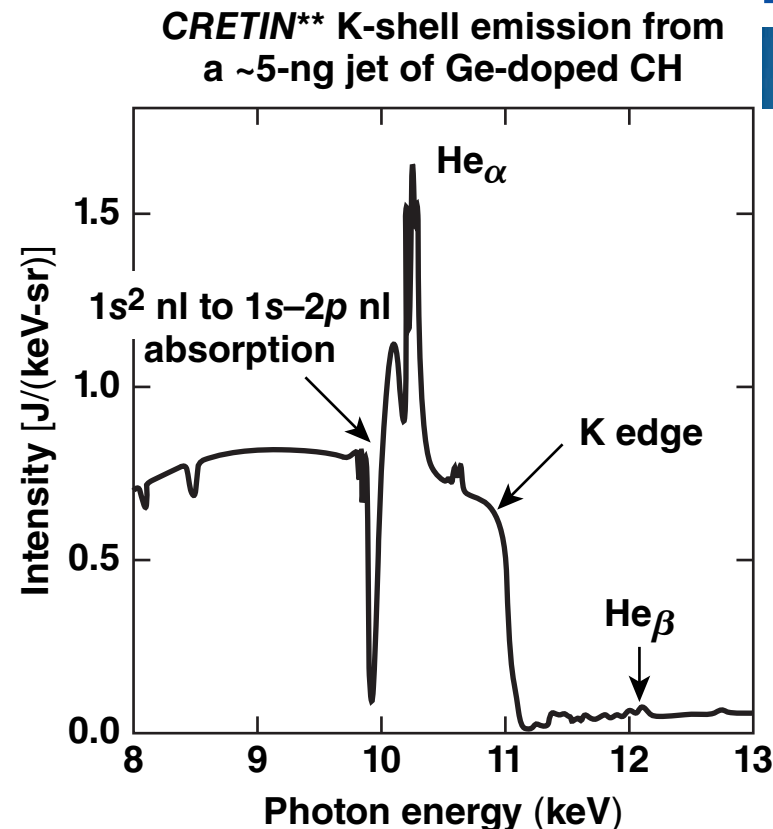
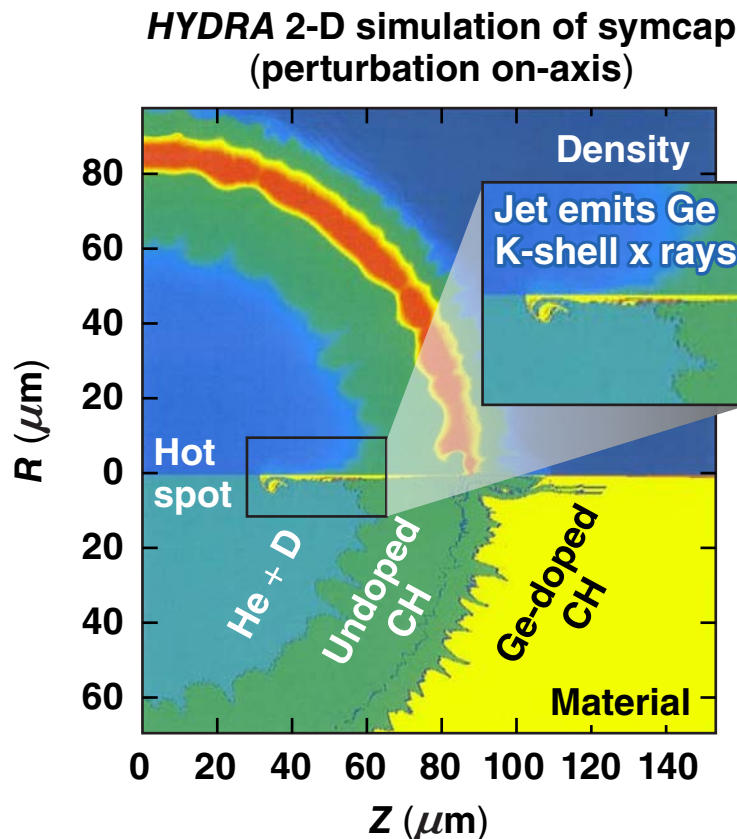
Ablative instability affects CH (Ge,Si)



Deceleration-phase instability affects CH (Cu)



Two-dimensional simulations predict bubbles of material from the ablation surface are mixed into the hot spot (hot-spot mix)*



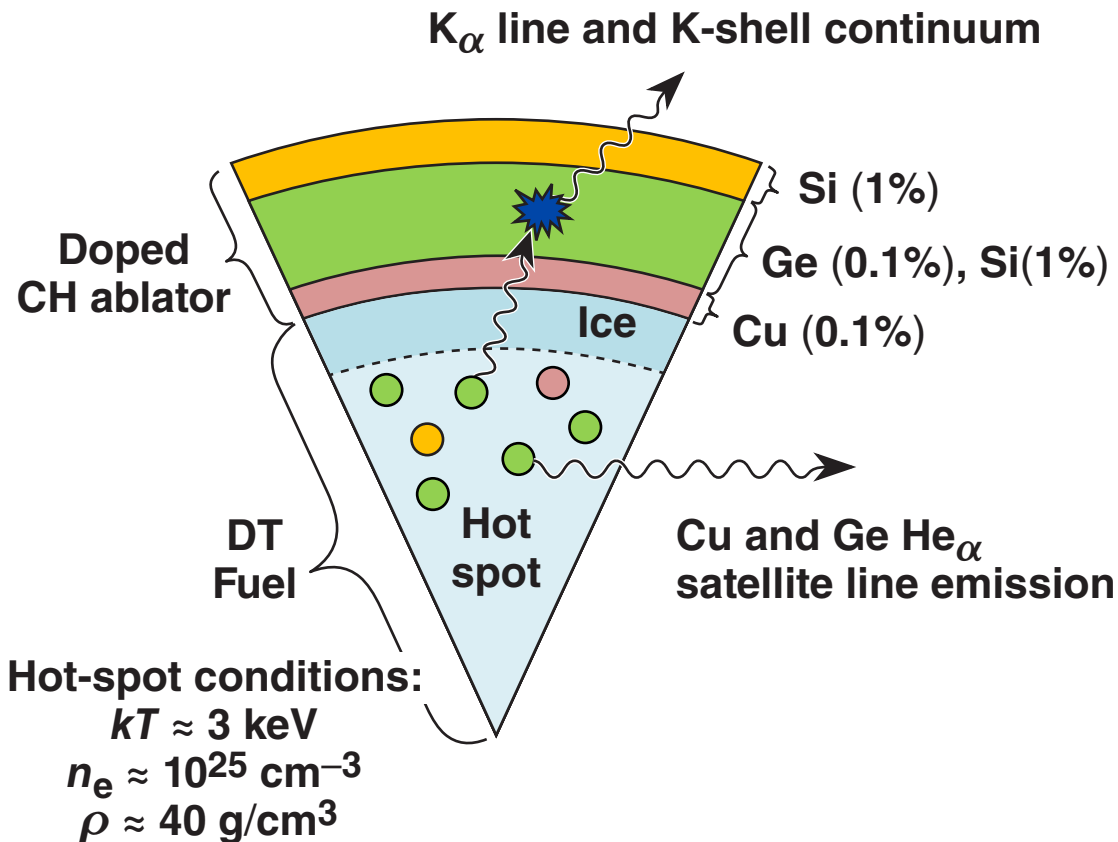
The symcap target replaces the DT cryo layer with a CH surrogate layer.

TC10707a

*B. A. Hammel et al., High Energy Density Phys. **6**, 171 (2010).

H. A. Scott, J. Quant. Spectros. Radiat. Transf. **71, 689 (2001).

Hot-spot mix and compressed-ablator ρR are diagnosed with x-ray spectroscopy near peak compression



- Mix from the ablation surface instability¹⁻³ →
 - Ge hot-spot emission
- Mix from the ablator/fuel interface¹⁻³ →
 - Cu hot-spot emission

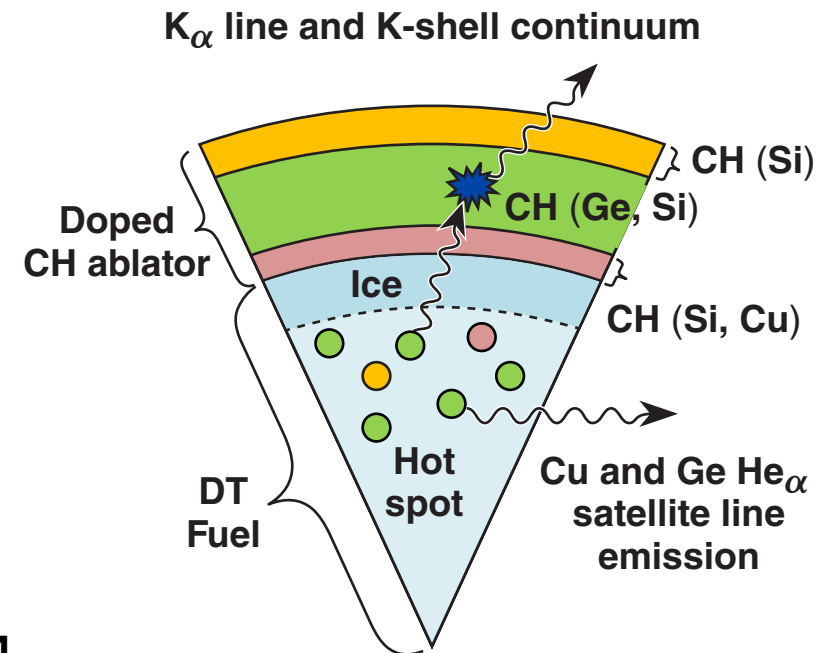
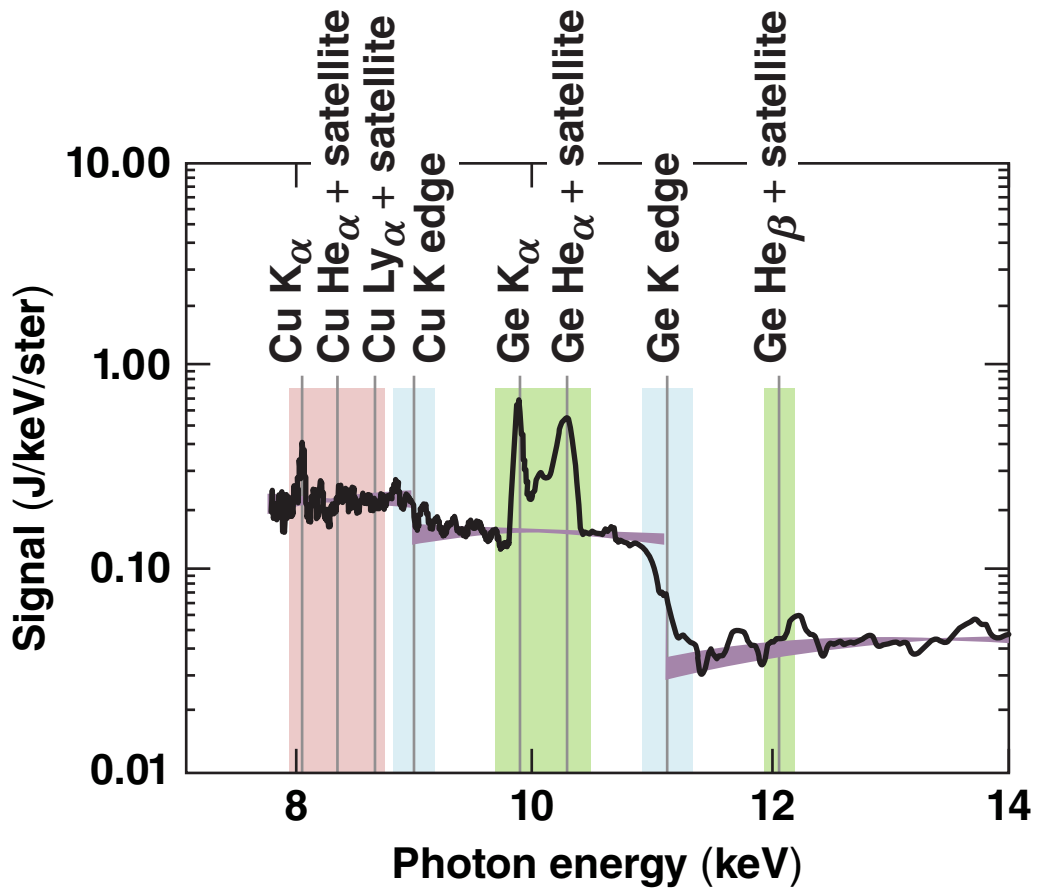
- X-ray continuum from the hot spot is attenuated by the K edges of dopants in the compressed ablator

¹B. A. Hammel *et al.*, High Energy Density Phys. **6**, 171(2010).

²S. W. Haan *et al.*, Phys. Plasmas **18**, 051001 (2011).

³S. P. Regan *et al.*, Phys. Rev. Lett. **111**, 045001 (2013).

The calibrated, spatially integrated x-ray spectrum contains features from the hot spot and the shell



Strong Ge features and weak Cu features are observed.

The mix mass is estimated from the brightness of the Ge and Cu He α + satellite emission, assuming uniform plasma conditions



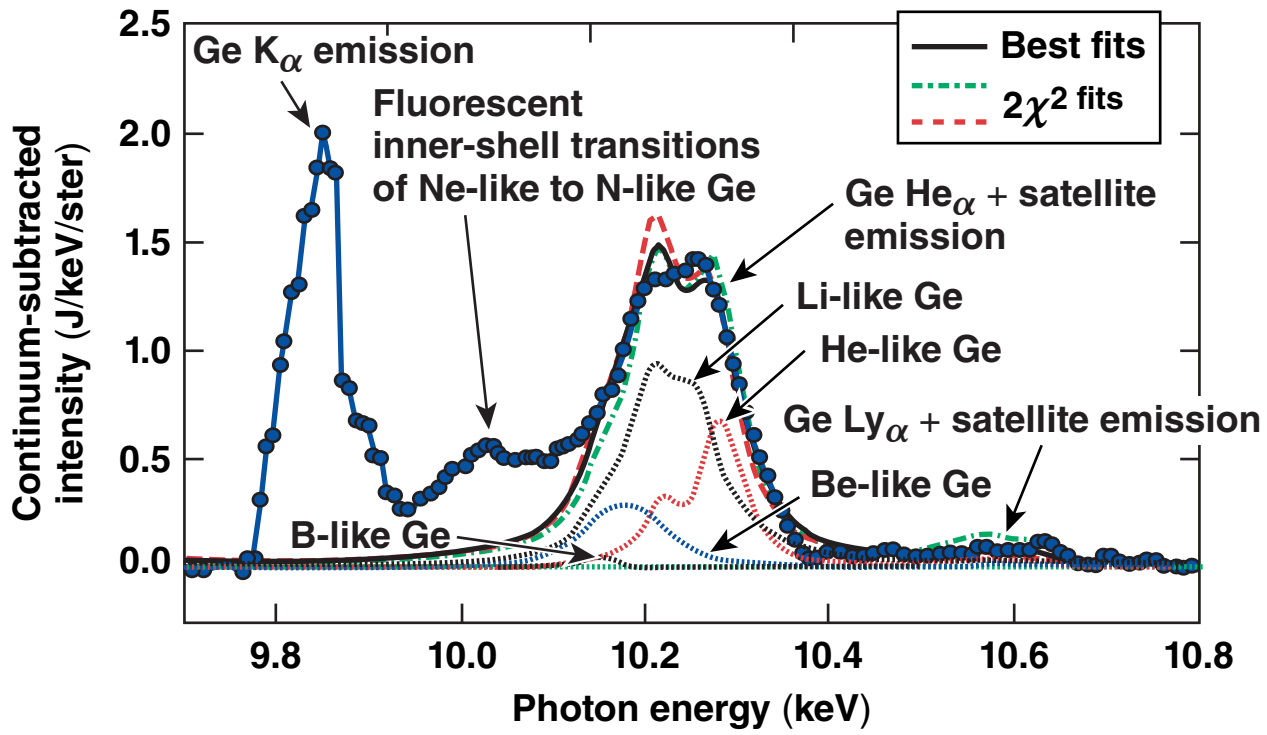
- The total time and spectrum-integrated line emission $\iint \langle P_{21}(h\nu) \rangle_{\text{meas}} dh\nu dt$ is measured
- The total line emissivity per ion $\langle p_2(T, \rho, R) A_{21} E_{21} \rangle$ is obtained from *PrismSPECT** as a function of T , ρ , and the average photon escape path length R .
- The total number of Ge ions under steady uniform conditions

$$N_{\text{Ge}} = \frac{\iint \langle P_{21}(h\nu) \rangle_{\text{meas}} dh\nu dt}{\langle p_2(T, \rho, R) A_{21} E_{21} \rangle \Delta t}$$

and the initial Ge atomic concentration give the total mix mass M .

Fitting the emission model to the data produces significant estimates of the three independent parameters T , ρ , and R .

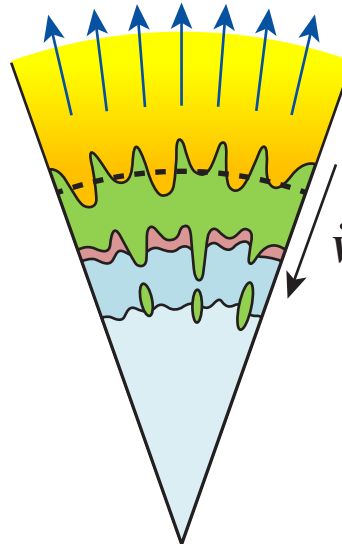
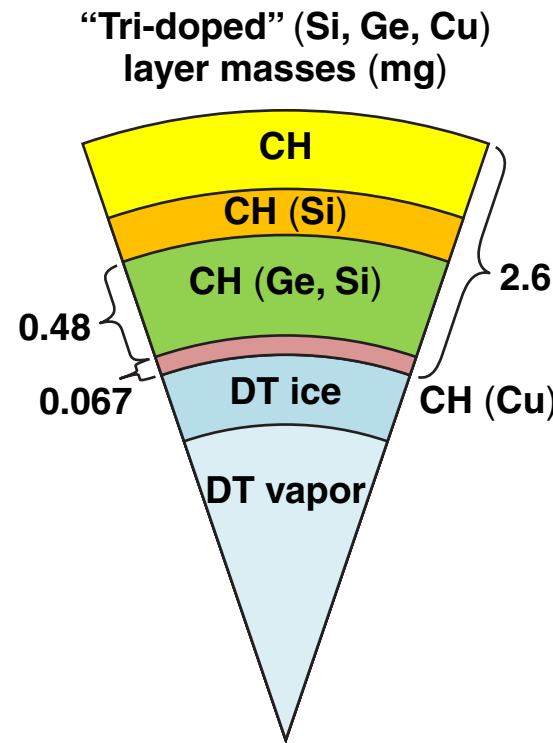
The spectrum is fit to the model to infer the hot-spot mix mass



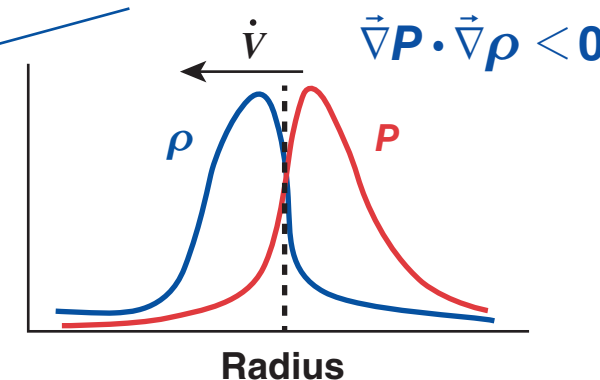
- $n_e = 0.9 (+0.1, -0.5) \times 10^{25} \text{ cm}^{-3}$
- $T_e = 3.0 (+0.6, -0.4) \text{ keV}$
- $\rho R_{\text{Ge}} = 0.325 (-0.1, -0.025) \text{ mg/cm}^2$
- $M_{\text{CH}} (\text{Ge, Si}) = 34 (-13, +50) \text{ ng}$
- $M_{\text{CH(Cu)}} < 2 (-1, +1) \text{ ng, upper limit}$

The Ge-doped mix mass is at least 17× more than the Cu-doped mix mass.

The ablation-front instability is primarily responsible for hot-spot mix*

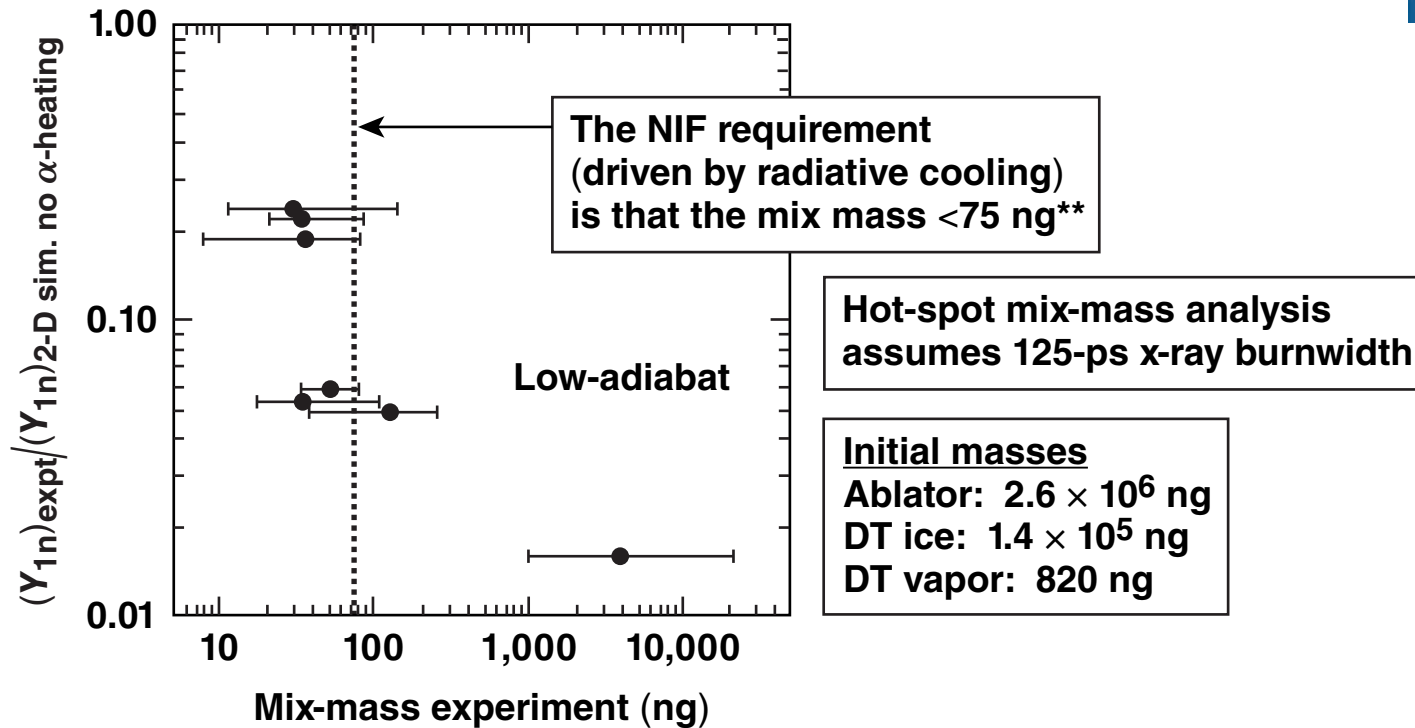


Ablative instability



The CH(Ge) mass is 7× the CH(Cu) mass, but at least 17× more CH(Ge) mix mass than CH(Cu) mix mass was observed.

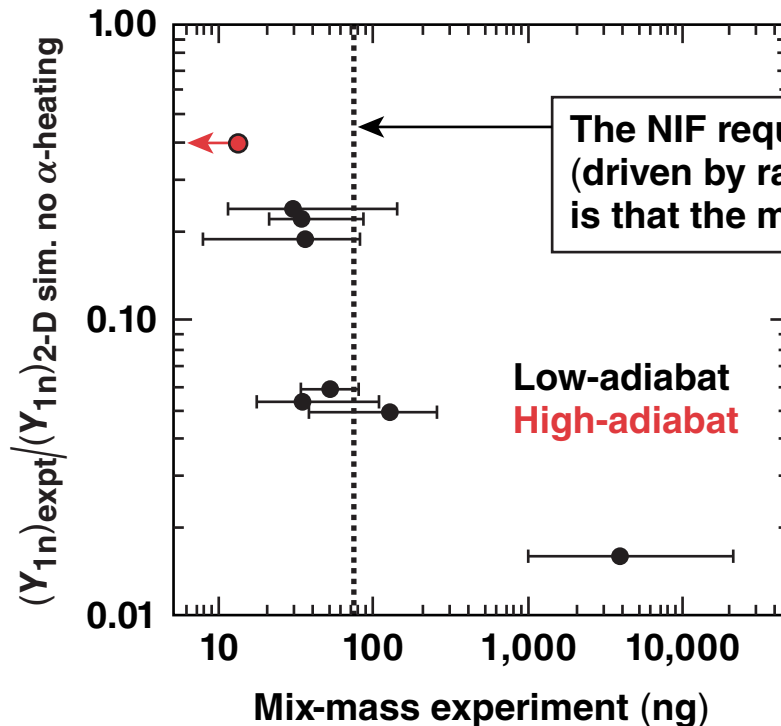
Low neutron yields and hot-spot mix mass around the 75-ng limit are observed*



*S. P. Regan et al., Phys. Rev. Lett. **111**, 045001 (2013).

S. W. Haan et al., Phys. Plasmas **18, 051001 (2011).

Less hot-spot mix and higher neutron yields are observed for the high-adiabat* implosion



J. S. Park et al., Phys. Rev. Lett. 112, 055001 (2014).

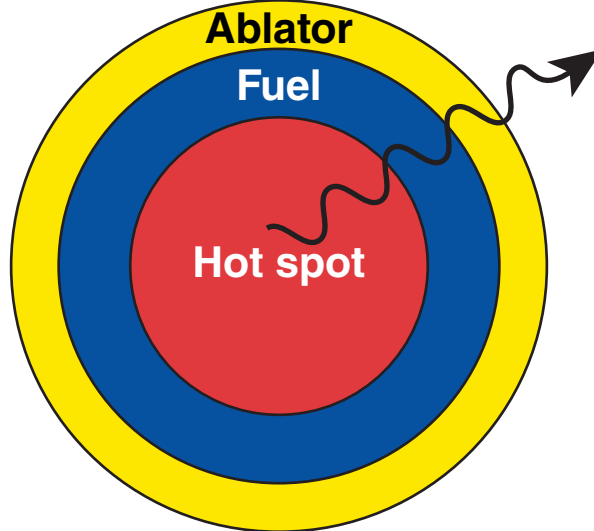
****S. W. Haan et al., Phys. Plasmas 18, 051001 (2011).**

***T. Ma et al., Phys. Rev. Lett. 111, 085004 (2013).

High-Z dopants are used to diagnose the compressed ablator near stagnation



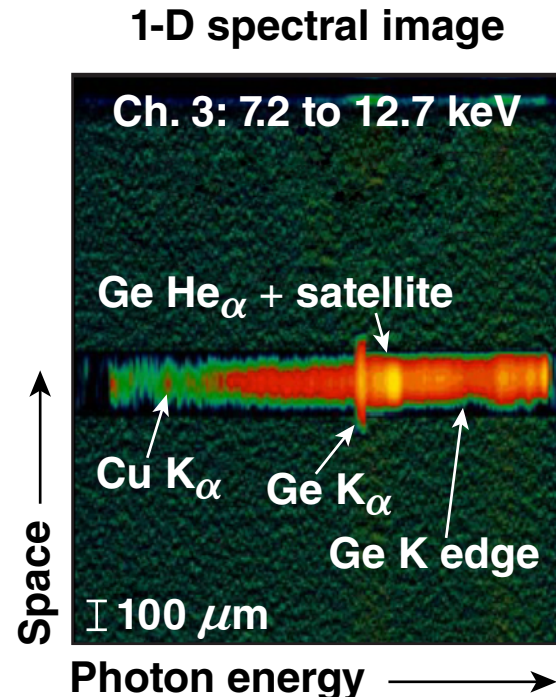
Compressed target at stagnation



$$I \propto e^{-h\nu/kT} e^{-\mu_{Ge}(n_e, T_e) \rho R_{Ge}} e^{-\mu_{Cu} \rho R_{Cu}} e^{-\mu_{CH} \rho R_{CH}}$$

Hot-spot
backlighter Ge shell
attenuation Cu shell
attenuation CH shell
attenuation

Measured x-ray spectrum
around stagnation



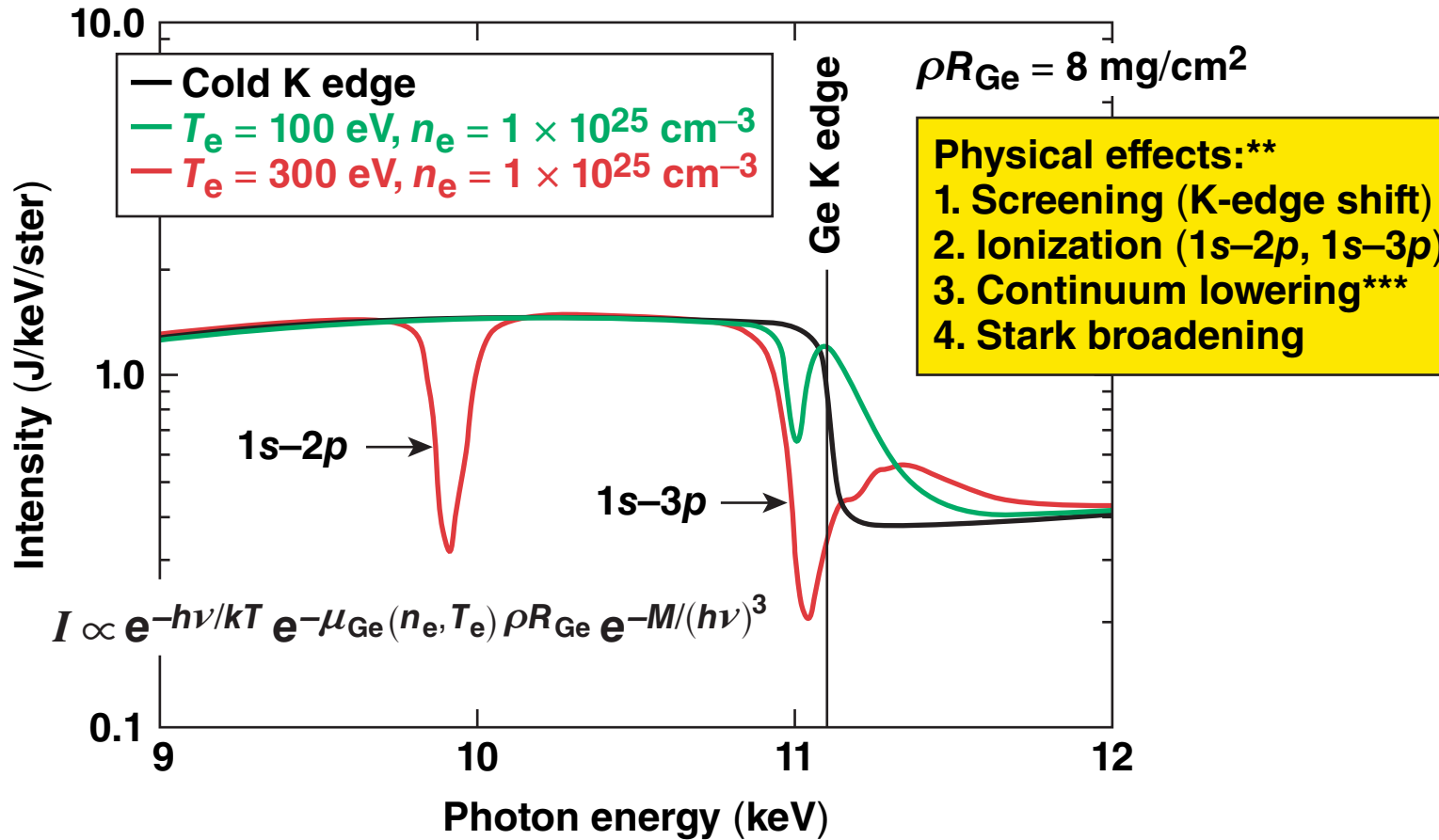
Adiabat: $\alpha \equiv P_{fuel}/P_{Fermi}$ (set by laser pulse shape)

E22511

The Ge opacity is sensitive to changes in n_e and T_e of the compressed ablator



Simulated emergent spectrum using *VISTA** opacity calculations



*B. G. Wilson and M. H. Chen, J. Quant. Spectrosc. Radiat. Transf. **61**, 813 (1999).

D. K. Bradley et al., Phys. Rev. Lett. **59, 2995 (1987).

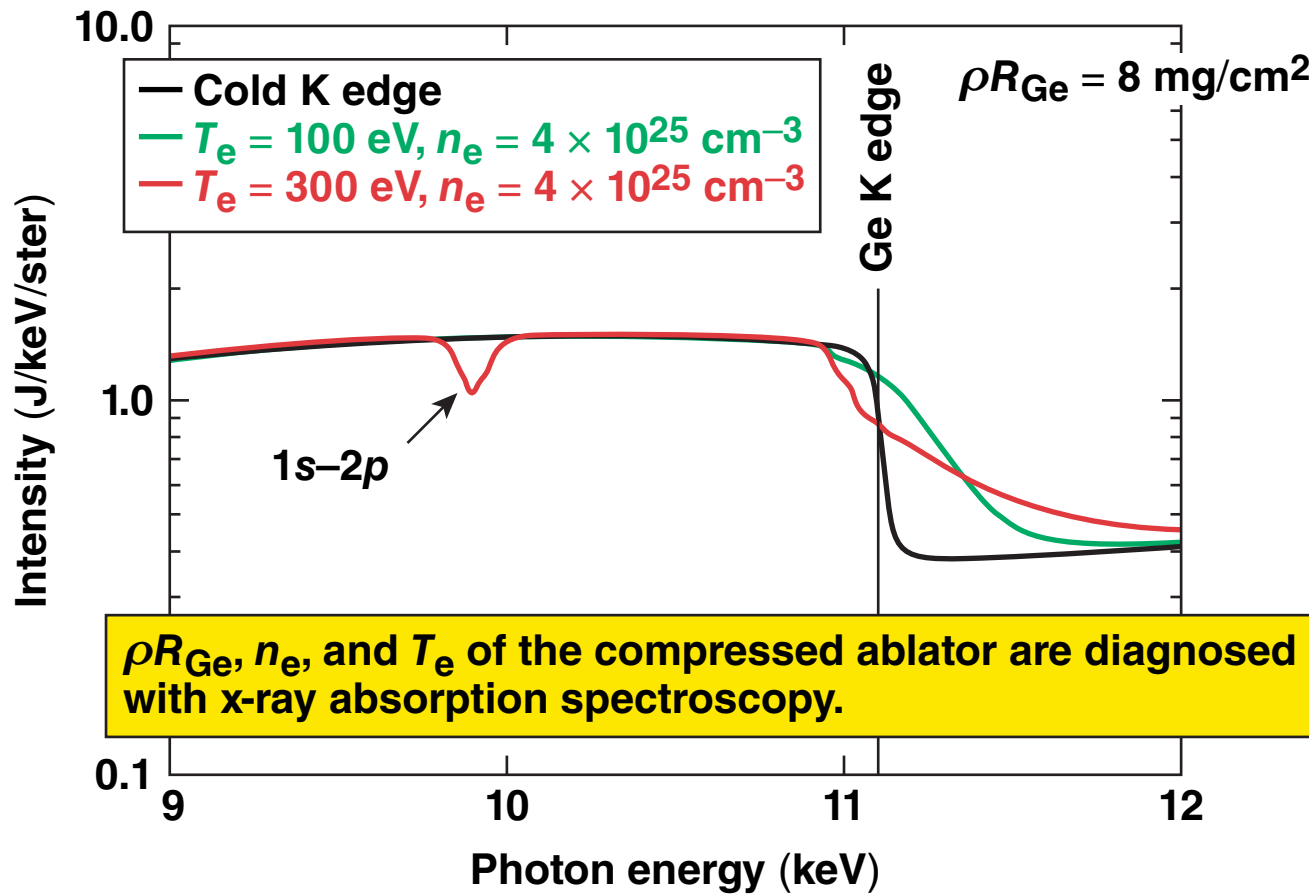
***J. C. Stewart and K. D. Pyatt, Jr., Astrophys. J. **144**, 1203 (1966).

E22638

Continuum lowering* reduces the 1s–3p and 1s–2p absorption features



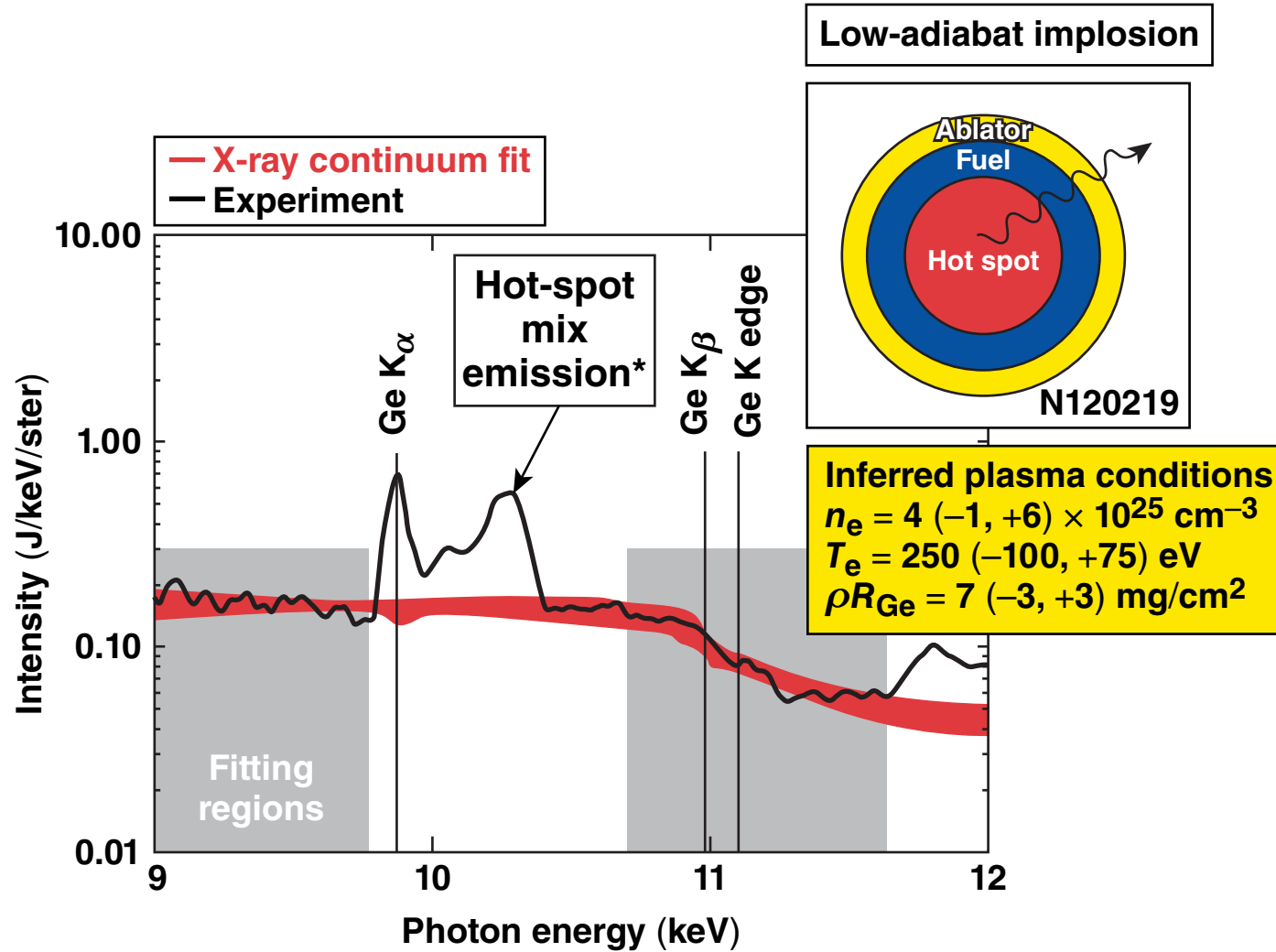
Simulated emergent spectrum using *VISTA*** opacity calculations



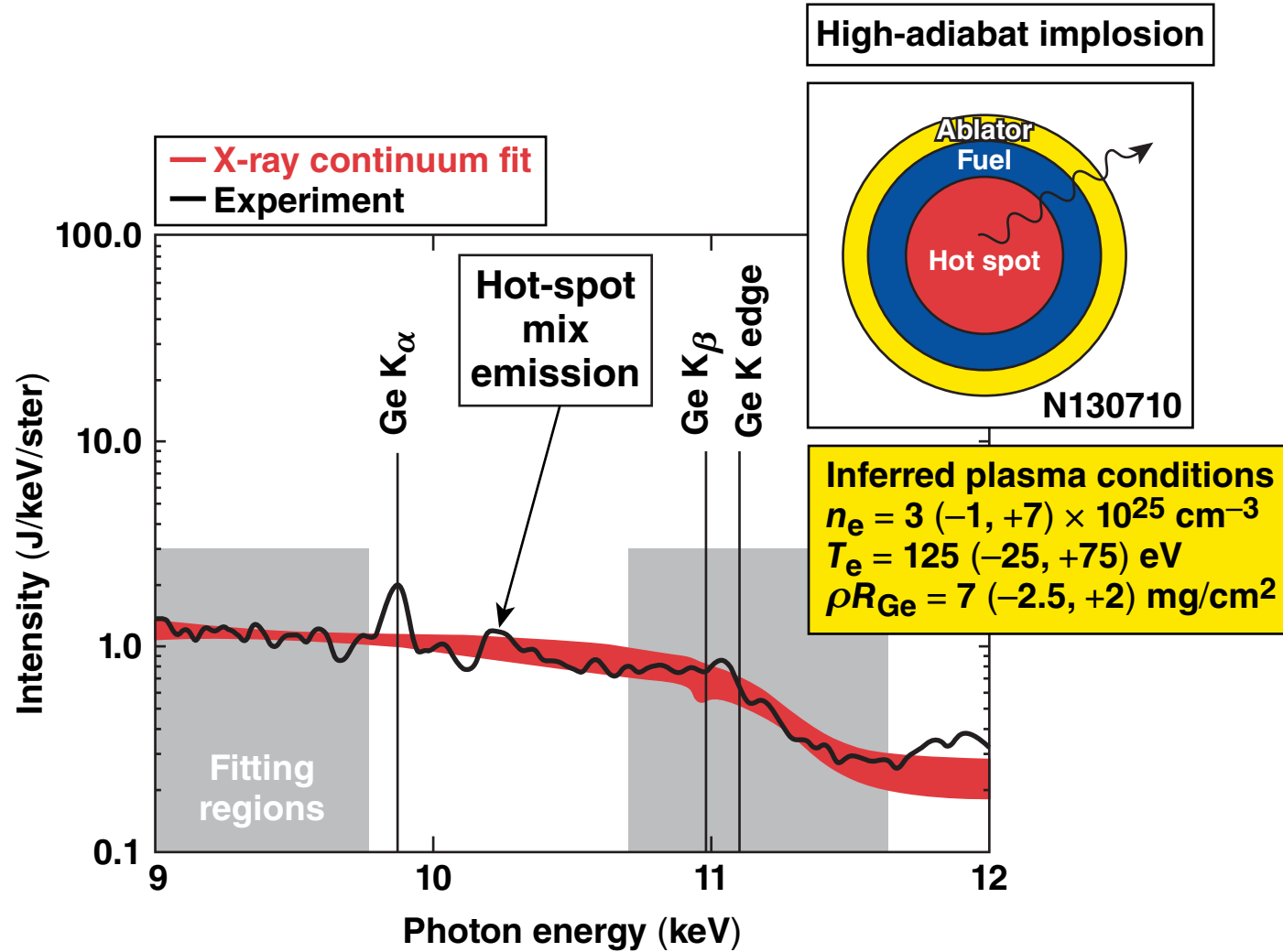
*J. C. Stewart and K. D. Pyatt, Jr., *Astrophys. J.* **144**, 1203 (1966).

B. G. Wilson and M. H. Chen, *J. Quant. Spectrosc. Radiat. Transf.* **61, 813 (1999).

A range of compressed plasma conditions is inferred for the low-adiabat implosion



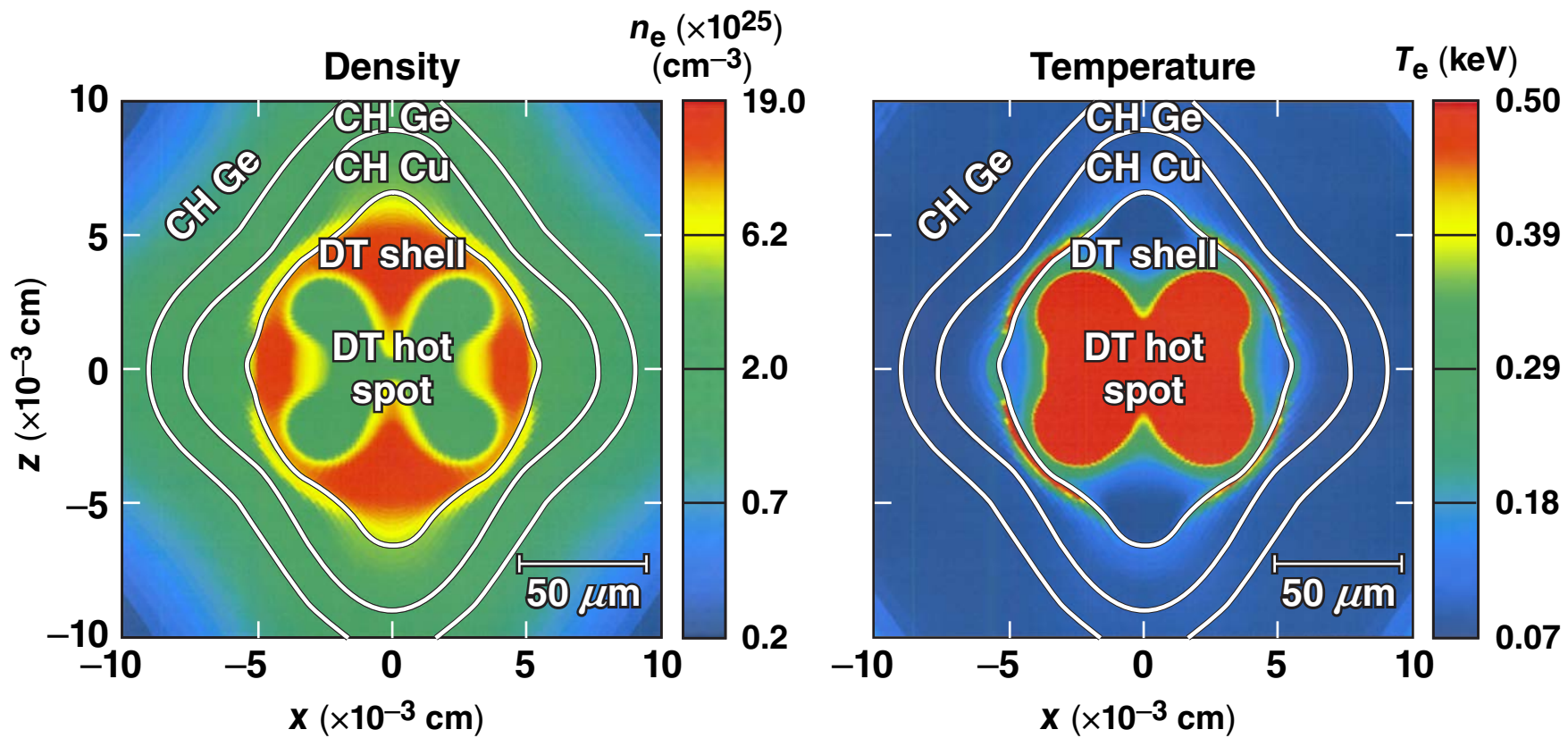
Similar analysis was performed for the high-adiabat implosion



Two-dimensional simulations show density and temperature in the DT-fuel layer is higher than in the compressed ablator



- 2-D HYDRA simulation of low-adiabat implosion near stagnation

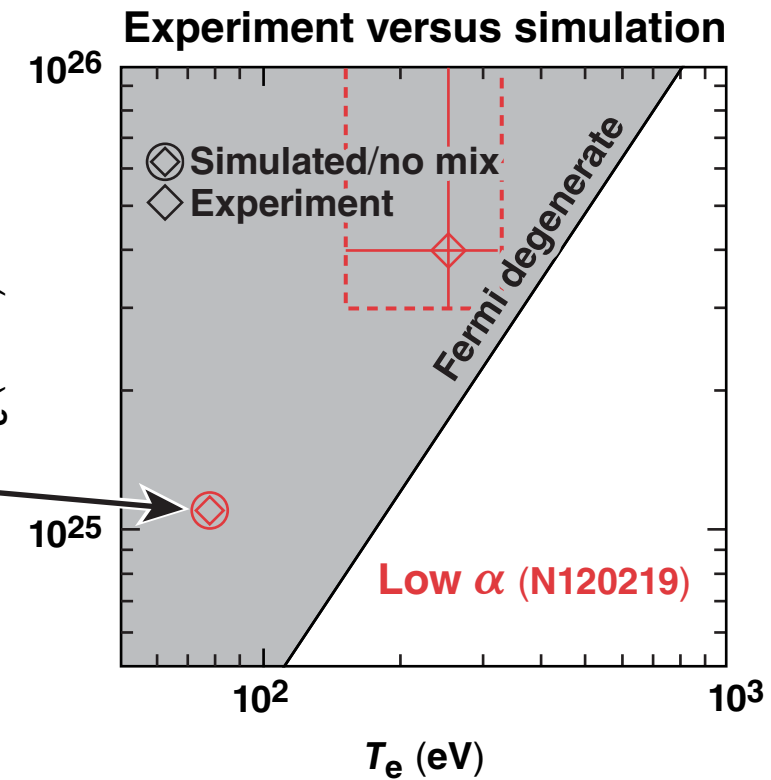
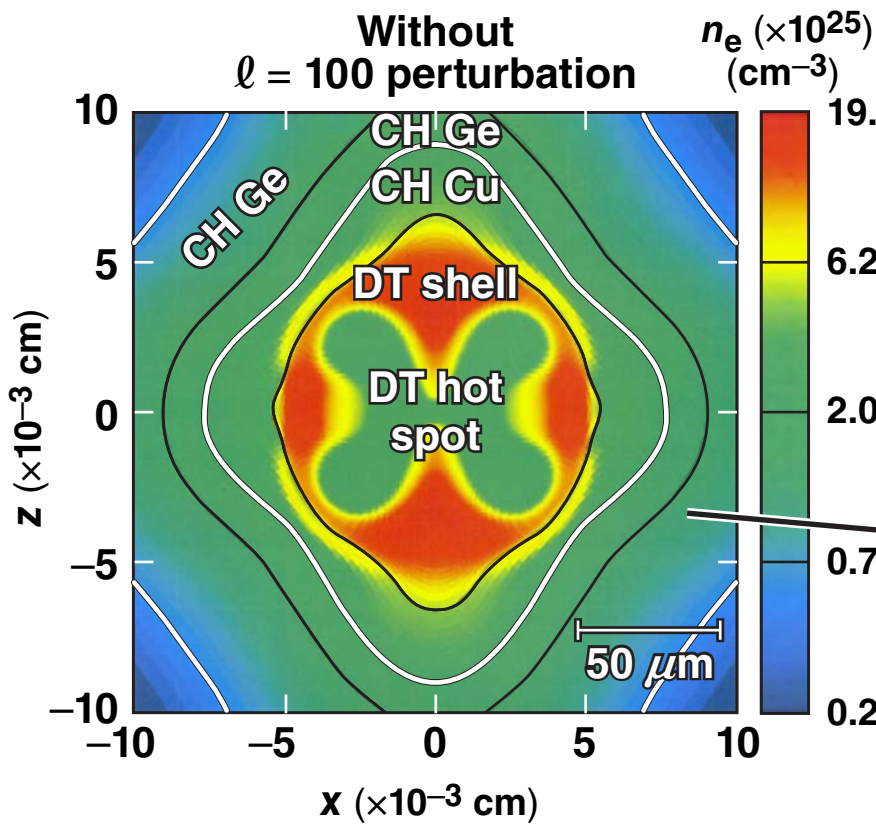


Simulated spatially and temporally averaged T_e and n_e of the compressed ablator are compared with the experimental results.

E23243

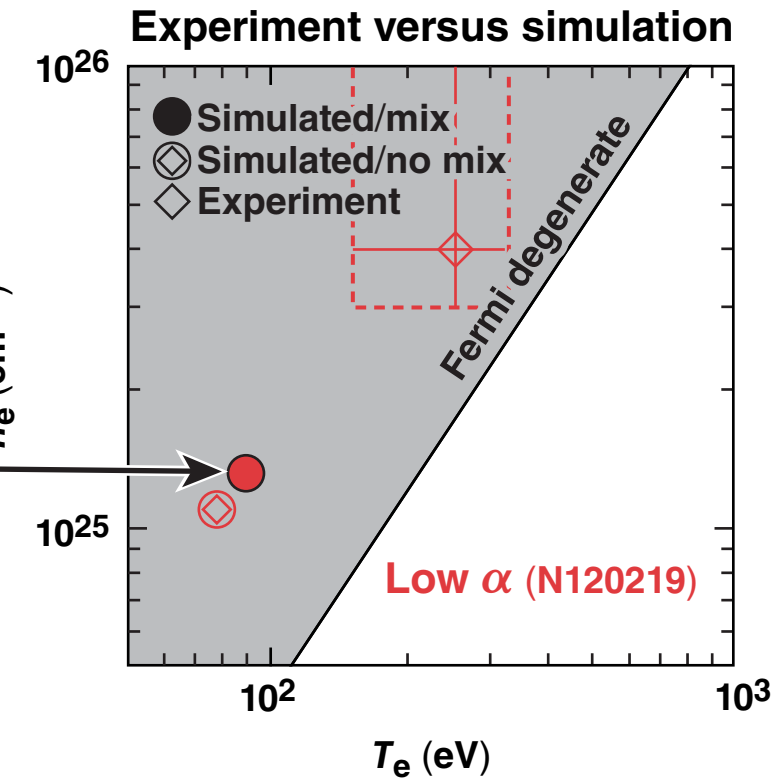
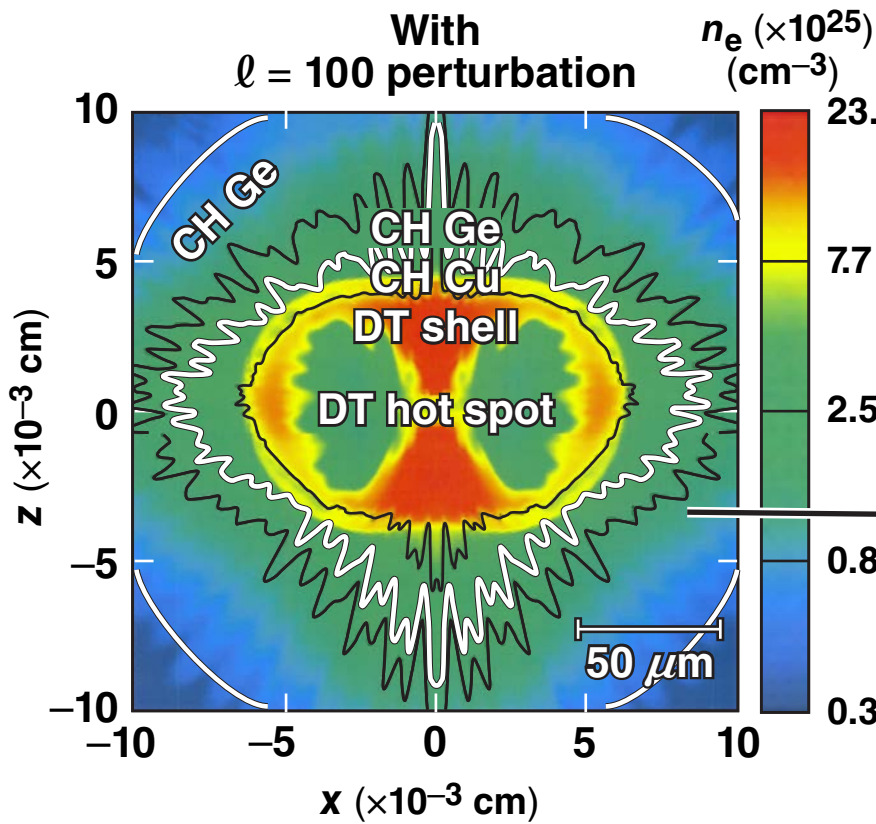
Simulated T_e and n_e of the compressed ablator without mix are much lower than the experiment

- 2-D HYDRA simulation of the low-adiabat implosion



The effects of hydrodynamic mixing of the target layers was explored with an $\ell = 100$ perturbation

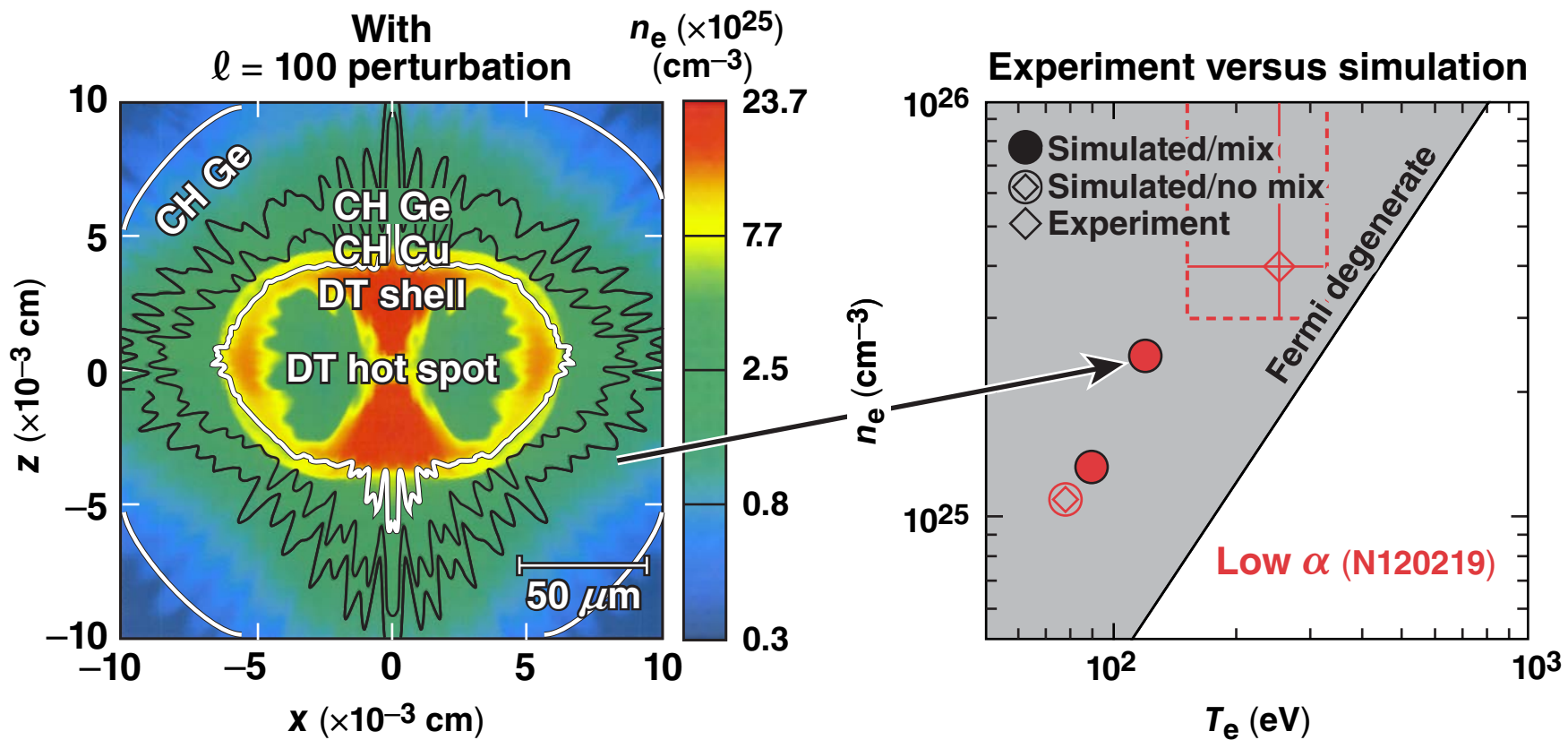
- 2-D HYDRA simulation of the low-adiabat implosion



The $\ell = 100$ mode perturbation slightly increases the simulated values.

Spatial average of simulated values over the entire compressed ablator is closer to experiment

- 2-D HYDRA simulation of the low-adiabat implosion

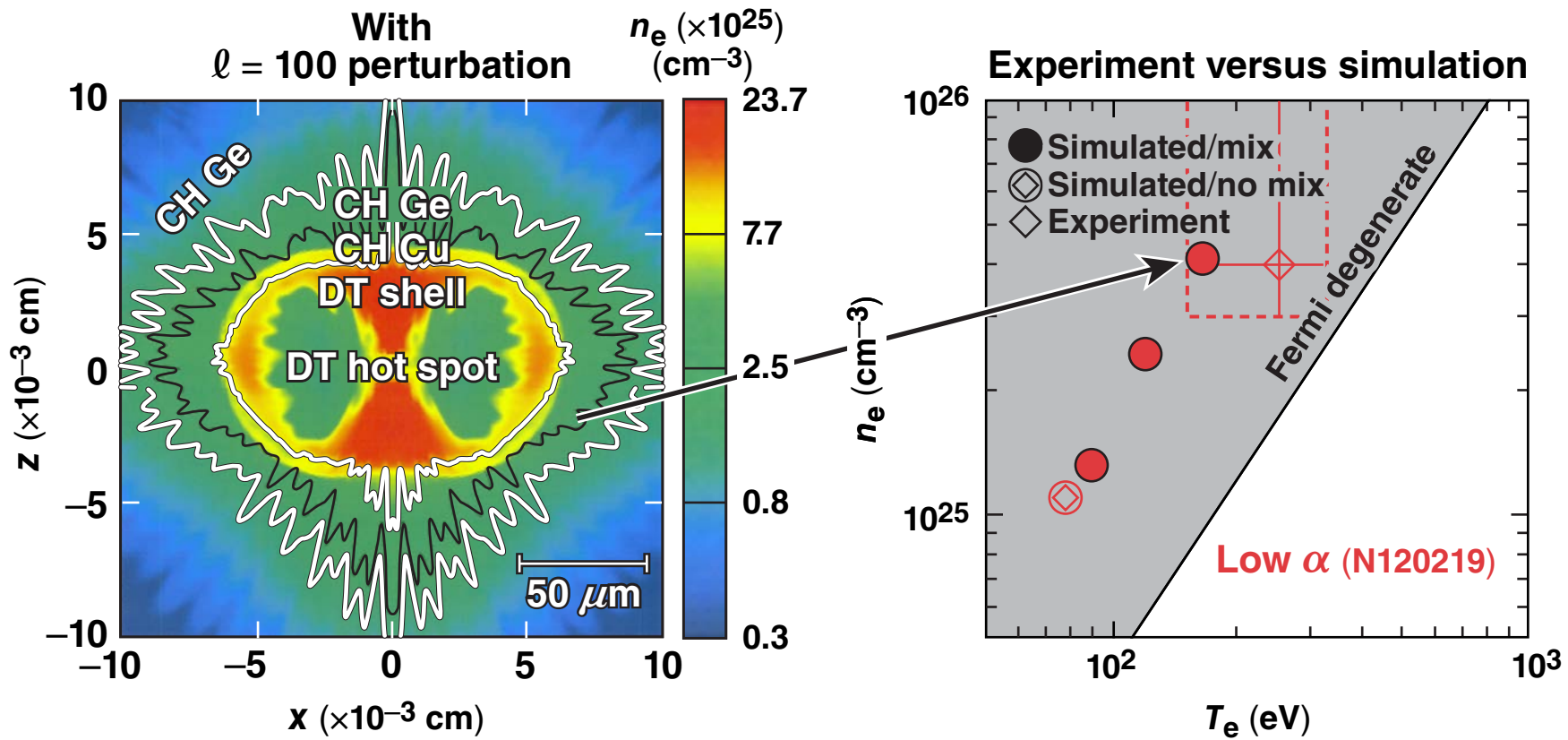


Significant mixing of CH(Ge) and CH(Cu) layers must occur.

Spatial average of simulated values over the inner compressed ablator is comparable to experiment



- 2-D HYDRA simulation of the low-adiabat implosion



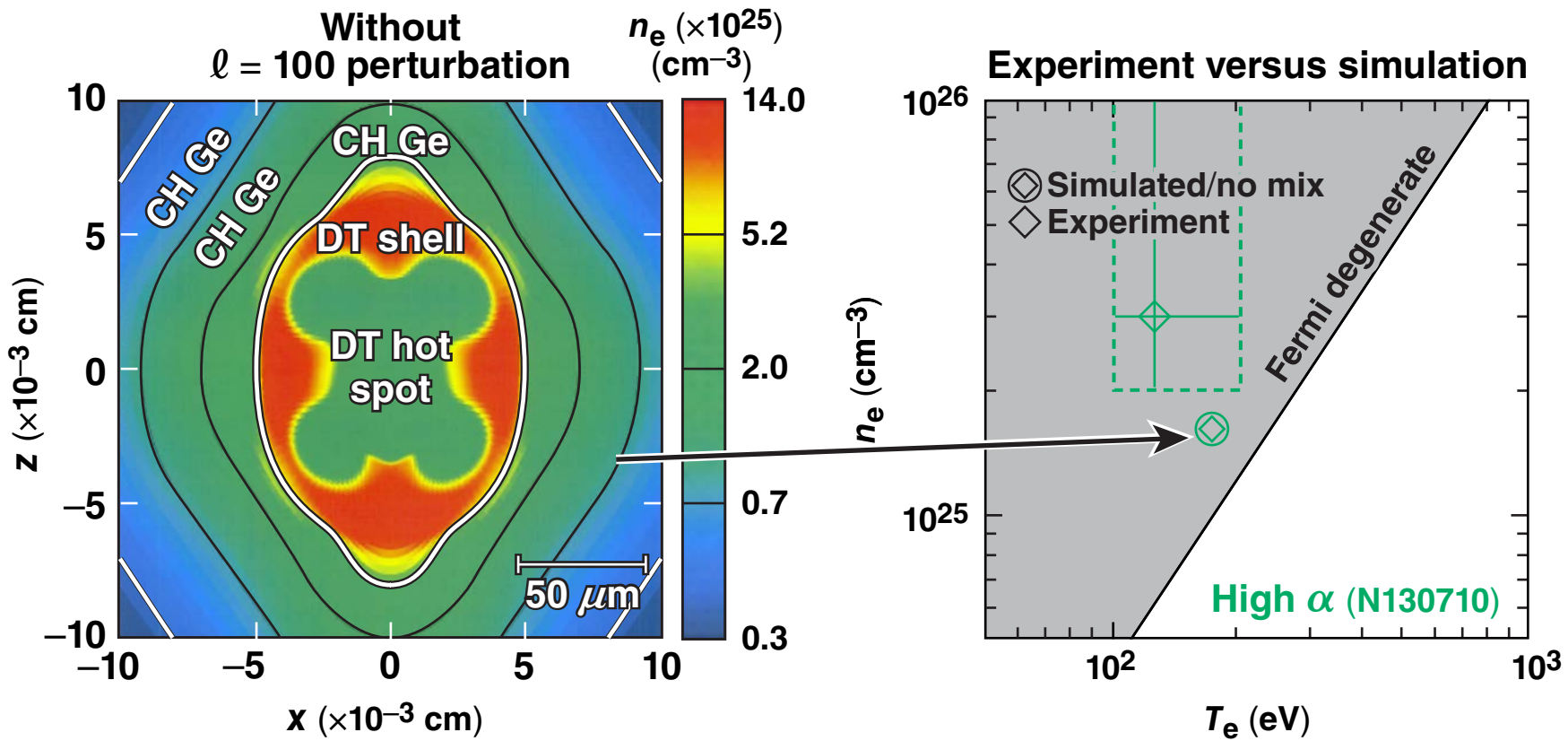
Measurement may be weighted to the highest T_e and n_e .

High-adiabat

The 2-D simulation without mixing for the high-adiabat implosion is close to the experimental result



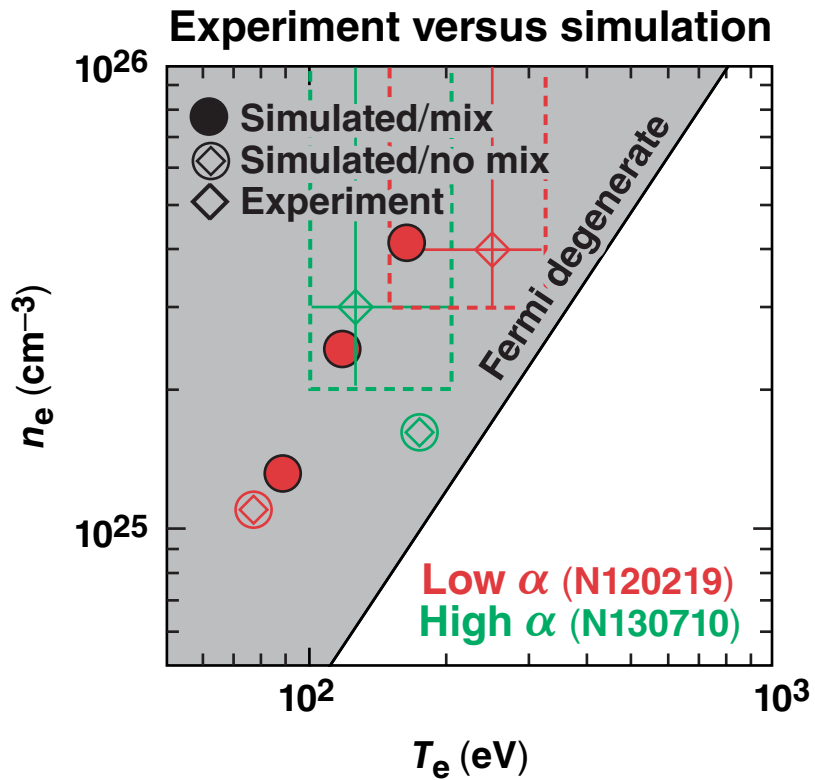
- 2-D HYDRA simulation of the high-adiabat implosion



Less hydrodynamic mixing of target layers is inferred for the high- α implosion compared to the low- α one.

E23248

Hydrodynamic mixing is predicted to increase the T_e and n_e of the Ge-doped CH in the compressed shell



The low-adiabat implosion has more hydrodynamic mixing of the target layers than the high-adiabat one.

Future direction

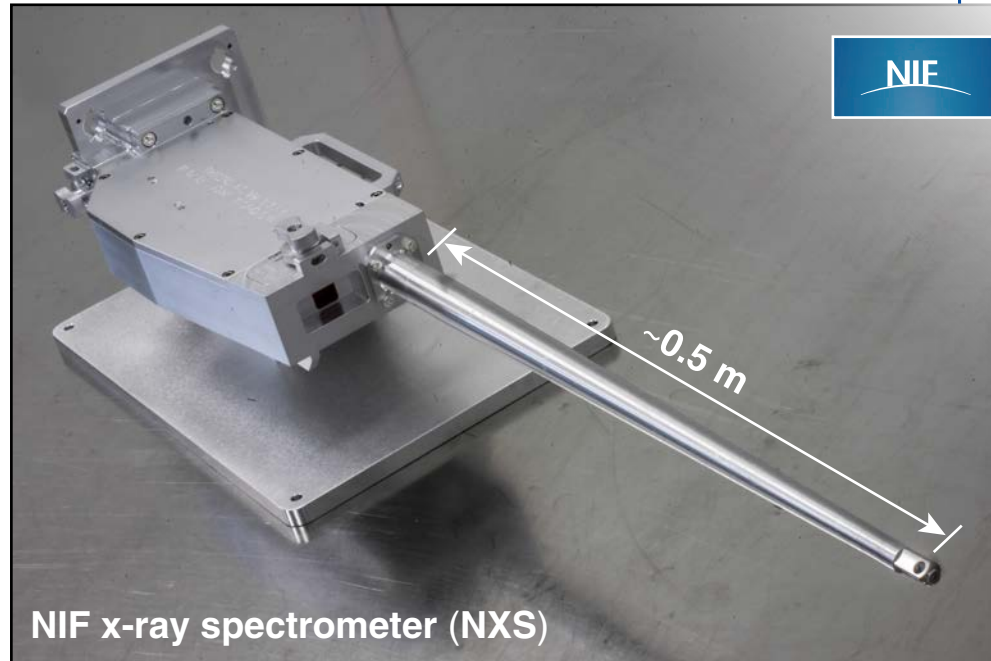
Time-resolved x-ray spectroscopy will be recorded on the NIF with the NXS



NXS/DISC

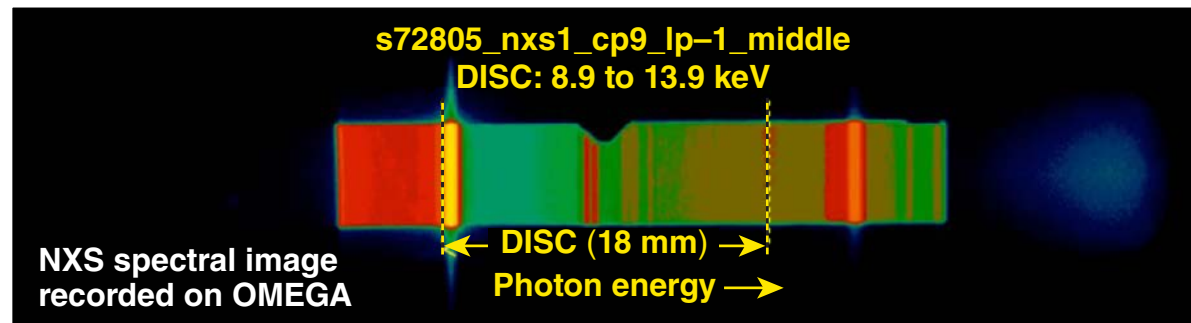
- Partially overlapping spectral windows in 2- to 18-keV range
- $E/dE \sim 100$
- $dt \geq 8 \text{ ps}$
- mm-scale x-ray sources
- absolute calibration

DISC = Diagnostic insertion manipulator imaging streak camera*



NIF x-ray spectrometer (NXS)

A time-integrated photometric calibration of NXS was performed on OMEGA



Performance qualification shot on the NIF was successfully completed on 3 June.

The hot-spot and compressed shell of ignition-scale implosions are diagnosed with x-ray spectroscopy



- Ablator mass mixed into the hot spot is inferred from the intensity of the $\text{He}_\alpha +$ satellite line emission of mid-Z ablator dopants*,**
- The origin of the hot-spot mix mass is investigated using Cu and Ge dopants placed at different radial locations in the ablator***
- The compressed-shell conditions are inferred from the absorption of x rays from the hot spot by the compressed Ge-doped CH
- Hydrodynamic mixing is predicted to increase the T_e and n_e of the Ge-doped CH in the compressed shell

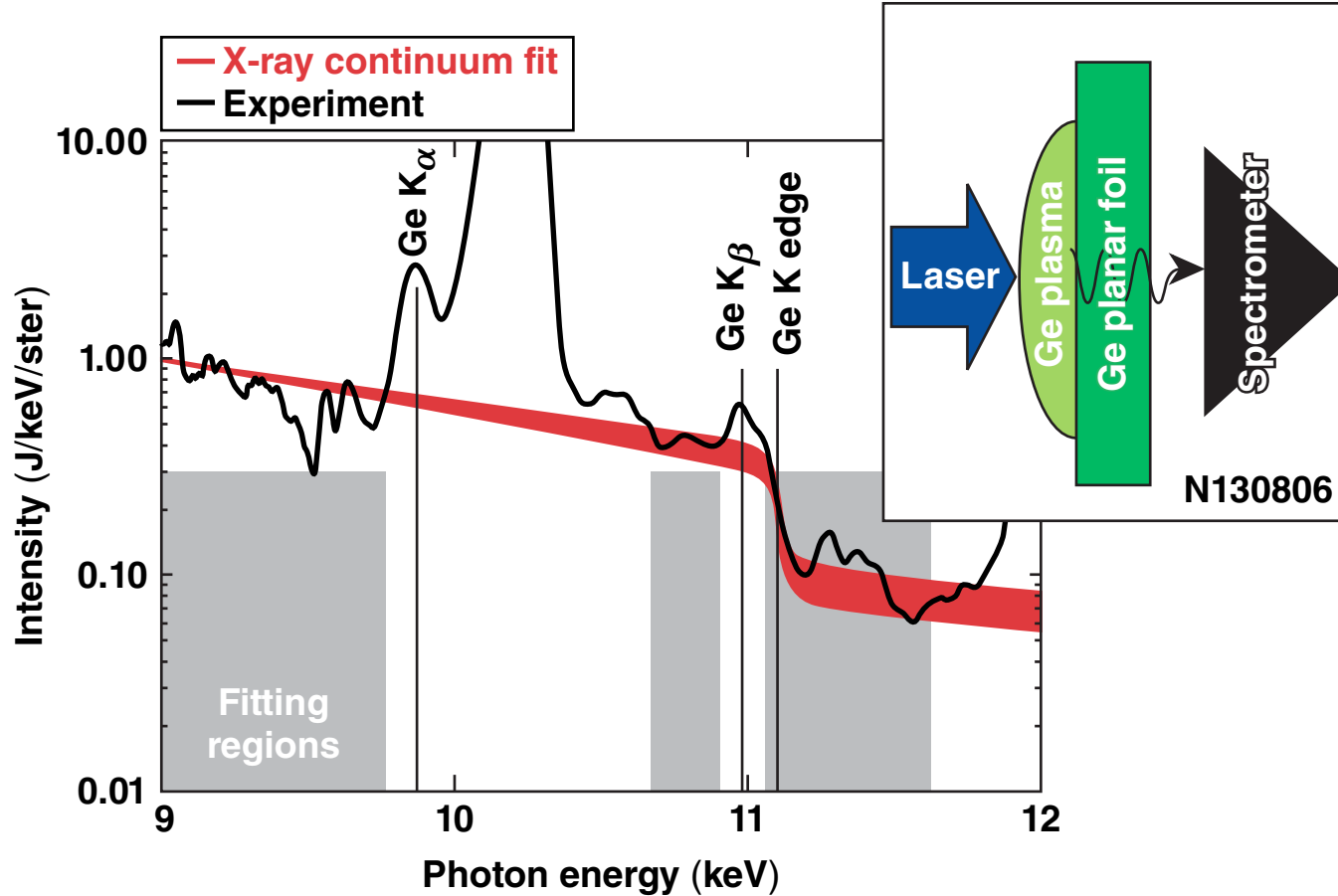
These time-integrated measurements will be extended with streaked x-ray spectroscopy using the National Ignition Facility (NIF) x-ray spectrometer (NXS).

*B. A. Hammel et al., High Energy Density Phys. 6, 171(2010).

**S. P. Regan et al., Phys. Plasmas 19, 056307 (2012).

***S. P. Regan et al., Phys. Rev. Lett. 111, 045001 (2013).

The cold Ge K edge was measured using a laser-driven, planar Ge target



$\rho R_{\text{Ge}} = 8.3 \text{ } (-2.8, +0.1) \text{ mg/cm}^2$ is inferred from this calibration shot using the cold opacity.*

The “ He_α ” feature is composed of $2p-1s$ transitions from L-shell ionization species

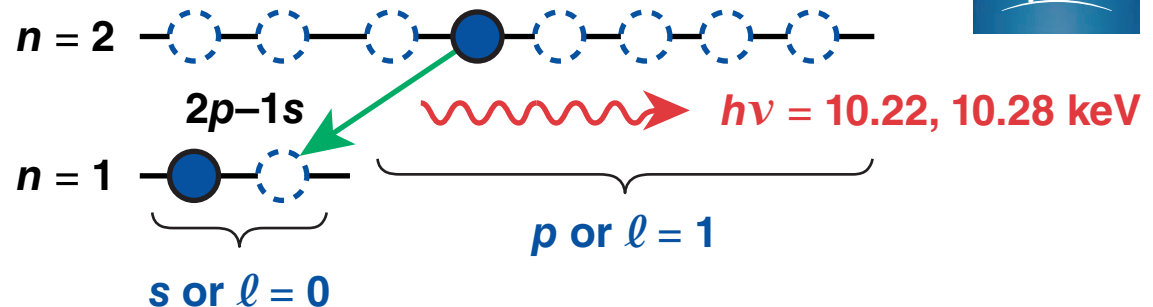


Core conditions:

$kT \approx 2 \text{ keV}$

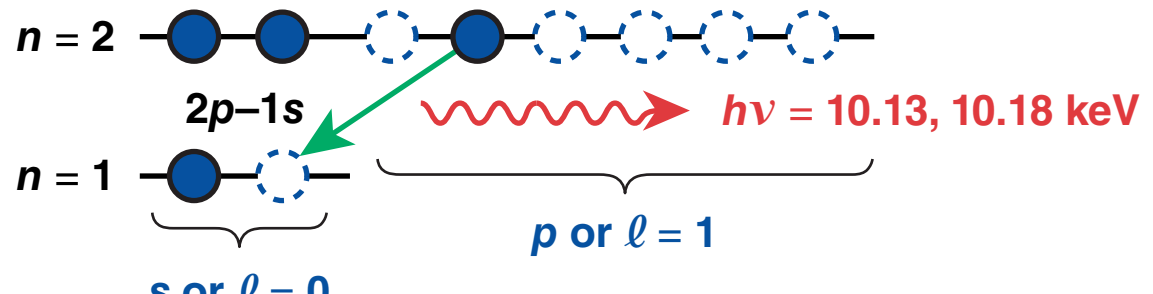
$Z \approx 26$ (C-like) through
30 (He-like)

He_α resonance and
intercombination lines



Be-like satellites of the
 He_α resonance lines

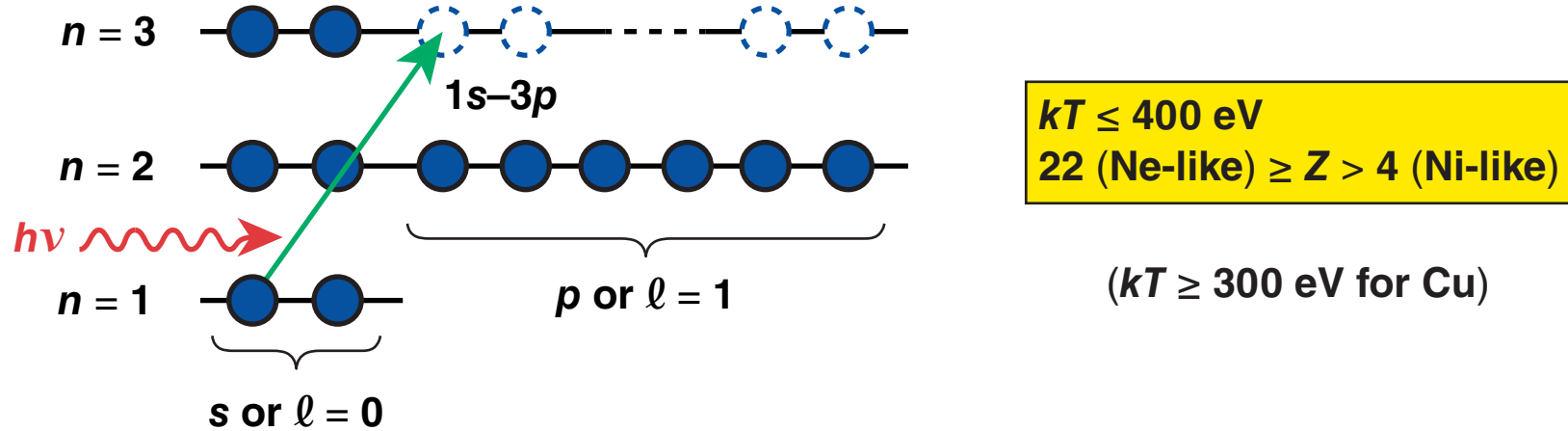
Autoionizing states are
formed primarily by
dielectronic recombination.



The 1s–2p absorption lines of Ge in the ablator are visible only for $Z > 22$ or for $kT > 400$ eV

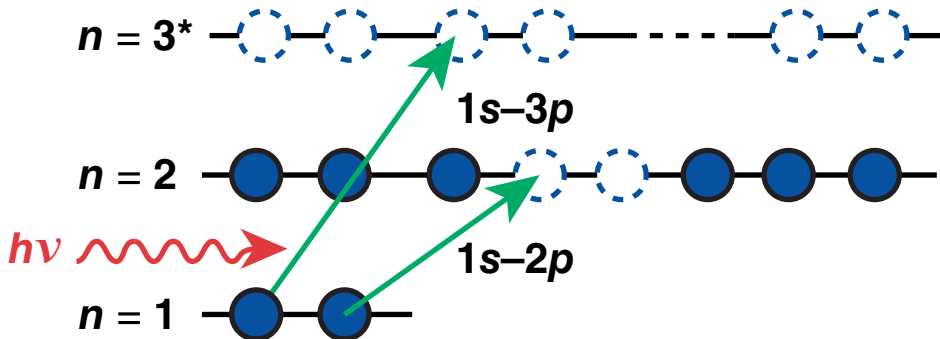


For 0.1% Ge in CH, $0.03 \leq \rho \leq 3$ g/cm³



$kT \geq 400$ eV
 $Z > 22$ (Ne-like)

* $n = 3$ may be removed
by continuum lowering



PrismSPECT* is an atomic detailed configuration accounting (DCA) spectrum simulation and analysis tool



- The Ge model includes 10,205 levels from the Ne-like through fully stripped ionization species, selected from a database of 32,176 levels
 - single excitations through $n = 10$ and double excitations through $n = 3$
 - collisional and radiative excitations and decays, autoionization, and dielectronic recombination
- The key resonance-line-emitting configurations are “spin-orbit” split
- Radiation-transport effects are calculated self-consistently for homogeneous objects with an “escape-probability” model
- Measured spectra are compared with model spectra for 7068 combinations of n_e , T_e , and ρR_{Ge}
- Line profiles are obtained using a semi-empirical formulation by Hans Griem**

* J. J. MacFarlane et al., High Energy Density Phys. 3, 181 (2007).

**H. R. Griem, Phys. Rev. 165, 258 (1968).

Profiles of the critical H- and He-like spectral lines in *PrismSPECT** are obtained from the multi-electron radiator line (*MERL*) code**

